Mercury evidence for pulsed volcanism during the end-Triassic mass extinction

Published in PNAS 2017 vol. 114 no. 30 , 7929–7934, doi: 10.1073/pnas.1705378114

L.M.E. Percival[1], M. Ruhl[1], S.P. Hesselbo[2], H.C. Jenkyns[1], T.A. Mather[1] and J.H. Whiteside[3]

1: Department of Earth Sciences, University of Oxford, South Parks Road, Oxford, U.K., OX1 3AN.

2: Camborne School of Mines and Environment and Sustainability Institute, University of Exeter, Penryn Campus, Penryn, Cornwall, U.K., TR10 9FE.

3: Ocean and Earth Science, National Oceanography Centre, University of Southampton, University Road, Southampton, U.K., SO17 1BJ.

ABSTRACT

The Central Atlantic Magmatic Province (CAMP) has long been proposed as having a causal relationship with the end-Triassic extinction event (~201.5 Ma). In North America and northern Africa, CAMP is preserved as multiple basaltic units interbedded with uppermost Triassic to lowermost Jurassic sediments. However, it has been unclear whether this apparent pulsing was a local feature, or if pulses in the intensity of CAMP volcanism characterized the emplacement of the province as a whole. Here, six geographically widespread Triassic–Jurassic records, representing varied paleoenvironments, are analyzed for mercury concentrations and mercury/total organic carbon (Hg/TOC) ratios. Volcanism is a major source of mercury to the modern environment. Clear increases in Hg and Hg/TOC are observed at the end-Triassic extinction horizon, confirming that a volcanically induced global mercury-cycle perturbation occurred at that time. The established correlation between the extinction horizon and lowest CAMP basalts allows this sedimentary mercury excursion to be stratigraphically tied to a specific flood basalt unit for the first time, strengthening the case for volcanic

mercury as the driver of sedimentary Hg/TOC spikes. Additional Hg/TOC peaks are also documented between the extinction horizon and the Triassic–Jurassic boundary (separated by ~200 kyr), supporting pulsatory intensity of CAMP volcanism across the entire province and providing the first direct evidence for episodic volatile release during the initial stages of CAMP emplacement. Pulsatory volcanism, and associated perturbations in the ocean–atmosphere system, likely had profound implications for the rate and magnitude of the end-Triassic mass extinction and subsequent biotic recovery.

Significance Statement

The end of the Triassic Period (~201.5 million years ago) witnessed one of the largest mass extinctions of animal life known from Earth history. This extinction is thought to have coincided with and been caused by one of the largest known episodes of volcanic activity in Earth's history. This study examines mercury concentrations of sediments from around the world that record this extinction. Mercury is emitted in gaseous form during volcanism, and subsequently deposited in sediments. We find numerous pulsed elevations of mercury concentrations in end-Triassic sediments. These peaks show that the mass extinction coincided with large-scale, episodic, volcanism. Such episodic volcanism likely perturbed the global environment over a long period of time and strongly delayed ecological recovery.

/body

1. Introduction

The end of the Triassic Period was marked by a major mass extinction event (~201.5 Ma; e.g. 1, 2), one of the five largest environmental perturbations of the Phanerozoic Eon. Significantly increased extinction rates of marine fauna, and major turnovers in terrestrial vegetation and vertebrate groups, have been well documented (e.g. 3–8). The end-Triassic mass extinction predated the onset of the Jurassic by ~100–200 kyr, as defined by the first occurrence of the Jurassic ammonite species *Psiloceras spelae* (9). The sedimentary record of the extinction correlates with a large (up to 6‰) negative excursion in organic-carbon isotopes ($\delta^{13}C_{TOC}$: Figure 1A), indicative of a severe carbon-cycle perturbation coincident with the biotic crisis (e.g. 10–13). Moroccan strata that record this global carbon-cycle perturbation are transected by the lowest documented flows of the Central Atlantic Magmatic Province (CAMP). Consequently, the end-Triassic

58 extinction has been postulated as precisely coincident with the onset of known CAMP volcanism (e.g. 2, 12,
59 14, 15).
60 CAMP represents the most aerially expansive continental Large Igneous Province (LIP) known on
61 Earth, consisting of volumetrically large-scale flood-basalt sequences covering at least 7×10^6 km^2 across four
62 continents and both hemispheres (Figure 2A: ref 16). In North America and Morocco, CAMP basalts are
63 interbedded with continental sediments that have precise temporal constraints and are stratigraphically well
64 correlated with marine sedimentary records (Figure 1A: refs 12, 14). The apparent episodic emplacement of
65 CAMP basalts over several 100 kyr, at least in Morocco and North America, is a key feature of this LIP.
66 The oldest known CAMP basalts are the lower Moroccan unit (termed the Lower Formation in the
67 High Atlas and the Tasguint Formation in the Argana basin: 17, 18). This unit is overlain by two further
68 Moroccan basalt units: the Middle and Upper Formations in the High Atlas (the former named the Alemzi
69 Formation in Argana: 17, 18). For clarity, the High Atlas names are used henceforth in this study. These three
70 basalt groups are interbedded with sedimentary deposits. A fourth extrusive unit, the Recurrent Formation, is
71 locally preserved higher in the Moroccan sequence, with much thicker sediments between it and the Upper
72 Formation (Figure 2B; 14, 17, 19). These four basalt units are defined and correlated on the basis of distinct
73 igneous geochemistry. Based on geochemical correlation with North American CAMP units, which are
74 temporally constrained by astrochronological and radioisotopic geochronology, the Moroccan Lower–Upper
75 Formations are thought to have erupted in quick succession, with several 100 kyr then passing before the
76 eruption of the Recurrent Formation (2, 14).
77 At least three major CAMP units are documented in North America: the Orange Mountain, Preakness,
78 and Hook Mountain Basalts in the Newark Basin (20), with time-equivalent basalts known from other North
79 American Basins. The Orange Mountain Basalt overlies thin, usually lacustrine, sediments deposited above
80 the extinction horizon, and is thought to have been extruded 14–20 kyr after that event (2, 14, 21).
81 Radioisotopic dating has demonstrated that the Preakness Basalt and Hook Mountain Basalt were emplaced
82 270 kyr and 620 kyr later, respectively (2). The Newark Basin Orange Mountain and Hook Mountain basalts
83 have been geochemically established as equivalent to the Moroccan Middle and Recurrent Formations,
84 respectively (14); the Preakness Basalts have no known Moroccan counterparts (2, 14). Consequently, North
85 American and Moroccan records suggest that CAMP was emplaced in at least three major pulses of basalt
86 extrusion over ~700 kyr, with the products of the first major pulse further divisible into at least three or four
87 geochemically and stratigraphically distinct units. Thus, a total of at least six CAMP units are documented in

88 Morocco/North America (Figure 2B), which were relatively close to one another at the end of the Triassic
89 Period. However, more geographically dispersed CAMP basalts are also known from southern Europe, Brazil,
90 and elsewhere in western Africa, with potentially different temporal relationships with the end-Triassic
91 extinction and the dated CAMP flows (16). Therefore, it is not clear whether the intensity of CAMP
92 volcanism was pulsatory across the entire province, or whether the apparent pulsing recorded in North
93 America and Morocco was a local feature of the much larger scale LIP.
94 Proxy records of volcanic volatiles can aid in reconstructing the history of CAMP volcanism and its
95 impacts. Analyses of pedogenic carbonates suggest increases in atmospheric pCO_2 following emplacement of
96 each of the Newark CAMP basalts (CAMP pulses 3, 5, and 6 in Figure 2B), supporting a pattern of globally
97 incremental emplacement (22). However, the effect of local processes, such as diagenesis, on this record
98 cannot be ruled out. Reconstructions of pCO_2 based on stomatal indices (albeit at low temporal resolution)
99 show no such pulsing during the Triassic–Jurassic transition (6, 23). Nor is there yet evidence of episodic CO_2
100 increases associated with the early Moroccan CAMP pulses (CAMP pulses 1, 3, and 4 in Figure 2B) that were
101 extruded coincident with, and in the immediate aftermath of, the extinction event.
102 Here, the volatile emissions and ocean-atmosphere impact of CAMP volcanism is investigated by
103 analysis of sedimentary mercury (Hg) concentrations across multiple Triassic–Jurassic sedimentary archives.
104 Volcanism is known to be a major natural source of mercury, emitting it as a trace volcanic gas (24). Gaseous
105 elemental Hg has a typical atmospheric residence time of 0.5–2 year (25), allowing the element to be globally
106 distributed before being drawn down and eventually deposited in sediments. Several Phanerozoic events have
107 previously been linked to approximately coeval LIPs through documented increases in sedimentary mercury
108 concentrations, including the end-Permian and end-Cretaceous extinctions and Toarcian Oceanic Anoxic
109 Event (e.g. 26–29). Importantly, sedimentary drawdown of Hg is typically achieved via organic matter (30,
110 31), although sulphides and clays may also play a role (32–34). Consequently, sedimentary Hg concentrations
111 are typically normalized against total organic carbon (TOC) to account for the effect on Hg drawdown by
112 changes in organic matter deposition rates when looking for evidence of an elevated supply of Hg to the
113 environment (26).
114 In addition to interrogating the pulsatory history of CAMP volatile emissions, mercury analysis of
115 uppermost Triassic sediments also provides a unique opportunity to test the assumption that Hg-enriched
116 sediments were deposited precisely coincident with the eruption of LIP basalts. There are excellent age
117 constraints on numerous end-Triassic records (including those containing CAMP basalts), and the precise

correlation between the end-Triassic extinction horizon and lowest Moroccan CAMP basalt (the Lower Formation) is well established. Such temporal constraints may allow some Hg/TOC peaks in uppermost Triassic sediments to be directly correlated with specific CAMP basalt units. This direct association between Hg/TOC excursions and specific basalt flows has not been possible for other events due to the poor preservation, or limited stratigraphic control relative to the sedimentary record, of many LIPs.

A recent study on the Triassic–Jurassic boundary section at New York Canyon (Nevada, USA) showed an abrupt increase in Hg concentrations and Hg/TOC ratios correlated with the negative excursion in $\delta^{13}C_{org}$ that marks the end-Triassic extinction horizon (35). These Hg excursions were attributed to volcanic processes operating during the emplacement of CAMP. Here, the New York Canyon results are greatly expanded by analyzing six further sedimentary records from around the world, to test whether the end-Triassic mercury perturbation was a global phenomenon. The possibility of multiple episodic peaks in sedimentary mercury is also investigated, to examine whether the documented pulsatory nature of CAMP emplacement occured province-wide, or was limited to specific areas of the LIP. The synchrony of any Hg excursions with respect to the earliest CAMP flows is also assessed using the established stratigraphic correlation between the end-Triassic extinction horizon and the stratigraphically lowest known CAMP basalts.

2. Study areas

End-Triassic records of both marine and terrestrial environments are known from a number of locations around the world (Figure 1 in ref 36). In this study, the mercury records from six geographically widespread sections are presented, representing a variety of marine and terrestrial paleoenvironments (Figure 2A): St Audries Bay (UK: restricted shallow-marine), Kuhjoch (Austria: open shallow-marine), Arroyo Malo (Argentina: back-arc shallow marine), Astartekløft (Greenland: fluvio-deltaic), Partridge Island (Canada: lacustrine), and Igounane (Morocco: evaporitic-lacustrine). See Supplementary Information S1 for details on all the studied sections, and Supplementary Figure S2 for a full correlation among all the above sections and other end-Triassic records.

3. Results and Discussion

3.1. Mercury as a recorder of CAMP volcanism

Clear excursions in Hg/TOC ratios and/or Hg concentrations are observed at five of the six studied locations (St Audries Bay, Kuhjoch, Arroyo Malo, Astartekløft, and Partridge Island). The onsets of these

excursions are stratigraphically coincident with the globally observed $\delta^{13}C$ negative excursion that marks the extinction horizon (Figure 3). Four sections also record additional peaks in Hg/TOC above that level. Crucially, at all sites where Hg has been normalized to TOC, the Hg/TOC peaks result from elevated Hg concentrations rather than decreased TOC content (see Supplementary Figure S4). For Partridge Island and Igounane sediments, Hg/TOC ratios were deemed unreliable due to the very low TOC content (typically below analytical uncertainty) in sedimentary samples. Consequently, Hg signals at these two locations are presented without normalization to TOC. The mercury trends generated in this study are also compared to the existing New York Canyon record (35) in Figure 3, which appears to have a subtly different trend in sedimentary Hg/TOC increase, potentially resulting from atmospheric or local sedimentological processes.

The observed peaks in sedimentary Hg and Hg/TOC strongly suggest that a perturbation to the global mercury cycle took place during the Triassic–Jurassic transition, beginning coincidentally with the end-Triassic extinction. The absence of a recorded mercury perturbation in sediments at Igounane is interpreted to result from their deposition being below the oldest known CAMP flows (thus at a time preceding the onset of CAMP basalt extrusion). A lack of change in terrestrial spores from Argana sediments below the CAMP basalts further suggest that these sediments were deposited prior to the end-Triassic extinction (14), and thus before the onset of CAMP volcanism.

The correlation between Hg excursions and the extinction horizon in the other five studied records is strongly suggestive of a perturbation to the global mercury cycle at that time. Variations in marine redox during the extinction may have influenced the marine Hg cycle, but the records at both Kuhjoch and Arroyo Malo do not show a consistent stratigraphic correlation between the observed Hg/TOC peaks and lithological or geochemical evidence for redox changes (37, this study). Additionally, the mercury excursions preserved in the terrestrial records from Astartekløft and Partridge Island could not have been caused by changes in the oceanic mercury inventory. Consequently, an atmospheric Hg perturbation is the most plausible cause.

The Hg perturbation also coincided with the established onset of an increase in atmospheric pCO_2, based on Hg/TOC and stomatal density records from Astartekløft (23: Supplementary Figures S2 and S5). This correlation suggests a geologically simultaneous increase in atmospheric Hg and CO_2, plausibly originating from magmatic degassing during CAMP emplacement. Emissions of both gases could also result

178 from thermogenic gas release from kerogen in subsurface organic-rich sediments intruded by (CAMP-
179 associated) sills. Thermogenic emissions have been previously suggested as a key contributor to LIP
180 atmospheric perturbations (e.g. 38, 39). Thermogenic volatiles also explain the observed negative excursion in
181 $\delta^{13}C$ at the extinction horizon more satisfactorily than magmatic carbon emissions (40). However, peaks in
182 Hg/TOC stratigraphically above the extinction horizon are not marked by distinct negative excursions in $\delta^{13}C$.
183 Consequently, there is less evidence for these later mercury perturbations resulting from thermogenic
184 emissions, and magmatic Hg emissions are a more probable cause.
185
186 Additional evidence for a volcanic origin of the perturbation to the global Hg cycle during the end-
187 Triassic extinction comes from the established correlation between the lowest known CAMP flow (the Lower
188 Formation in the High Atlas) and the extinction horizon. This correlation allows the Hg/TOC increase at the
189 extinction horizon to be precisely stratigraphically matched with that particular unit of CAMP (Figure 1B: see
190 also Supplementary Figure S2 and refs 14, 15). Consequently, it is highly likely that volcanic Hg associated
191 with this lowest CAMP flow contributed to the global mercury perturbation during the end-Triassic
192 extinction. The ability to correlate stratigraphically a Hg excursion directly with an individual CAMP basalt
193 flow greatly strengthens the use of this element as a proxy for volcanism.
194
195
196 *3.2. The pulsatory release of magmatic volatiles*
197 In addition to the mercury excursion at the extinction horizon, four sections record distinct peaks in
198 sedimentary Hg/TOC higher up in the stratigraphy. These higher peaks are most clearly distinct at Kuhjoch
199 and Arroyo Malo, but may also be recorded at New York Canyon and St Audries Bay (Figure 3). Pulsatory
200 CAMP volcanism has been inferred from the stratigraphic record of CAMP basalts in North America and
201 Morocco (17–20). However, these lithological records only prove an apparent pulsing of CAMP basalts in
202 specific locations of what is a much larger scale province. Episodic volcanism across the entire extent of
203 CAMP has been inferred from pedogenic carbonate pCO_2 reconstructions (22), but these concretionary
204 carbonates can be impacted by local (diagenetic) processes. The observed pulsatory signal of Hg perturbations
205 in multiple, globally distributed, sedimentary records across the Triassic–Jurassic transition provides
206 independent evidence that the intensity of CAMP volcanism, and likely CAMP emplacement, occurred in a
207 non-continuous manner.

Although the mercury records shown in Figure 3 do show excursions in Hg/TOC in Jurassic strata and support the continuation of CAMP volcanism into the Jurassic, most of the Hg/TOC peaks are documented between the end-Triassic extinction horizon and the Triassic–Jurassic boundary. The data (Figure 3) suggest that at least two, and possibly three, major volcanic episodes occurred between the extinction and the beginning of the Jurassic (as defined by ammonite biostratigraphy). This interval is estimated as lasting only 100–200 kyr based on U–Pb geochronology and astrochronology (e.g. 1, 2, 41, 42). Ar–Ar and U–Pb geochronology suggests that the oldest three Moroccan basalt units (the Lower, Middle and Upper Formations: units 1, 3, and 4 in Figure 2B) and the first of the major North American CAMP pulses (units 2–4 in Figure 2B) were likely all emplaced during this interval (2, 14, 17). It is possible that the observed three pulses in Hg/TOC observed in strata between the extinction horizon and the Triassic–Jurassic boundary may directly relate to atmospheric volatile release from the first three CAMP basalt units in the Moroccan Argana Basin, and their North American equivalents. However, further correlative work is needed to confirm such a hypothesis. The later North American CAMP basalts, and the Moroccan Recurrent Formation (units 5 and 6, Figure 2B), were emplaced 300–600 kyr after the extinction (2, 14, 21 and references therein). Thus, the Hg/TOC peaks between the extinction horizon and the Triassic–Jurassic boundary cannot be related to these later flows.

The observed record of multiple pulses in Hg/TOC is direct evidence that volatile release associated with CAMP volcanism was also pulsatory, likely including episodic emissions of carbon, sulfur, and mercury. Moreover, pulsatory emissions are shown to have occurred throughout the first 100–200 kyr immediately following the end-Triassic extinction, in addition to the documented later pulses of volcanic emissions (22). Consequently, the large increase in atmospheric pCO_2 during the extinction event may have arisen as a series of episodic carbon-cycle perturbations to the atmosphere (and subsequently the ocean). Pulsatory perturbations of the ocean–atmosphere system caused by episodic volcanic events (and release of volatiles) associated with CAMP may explain the documented prolonged period of ecosystem deterioration and delayed recovery of benthic fauna during the emplacement of CAMP (35, 43–45).

4. Conclusions

Investigation of the global history of CAMP volatile emissions is important for understanding the development of this igneous province and its potential environmental impact. This study demonstrates that the mercury cycle was perturbed on a global scale during the Triassic–Jurassic transition. Mercury excursions are recorded in five of the six sections studied; the one section with no record of Hg enrichment was likely deposited prior to the onset of CAMP volcanism. The onset of Hg enrichment occurred synchronously across the globe, coincident with the end-Triassic extinction and associated global carbon-cycle perturbation. The presence of Hg/TOC excursions in sedimentary records of terrestrial and marine paleoenvironments, across both hemispheres, indicates that atmospheric mercury concentrations likely increased substantially. This atmospheric perturbation probably resulted from the emplacement of CAMP and the associated large-scale emission of magmatic volatiles, and potentially thermogenic volatiles from intruded country rock (including mercury). The appearance of a global Hg excursion at the end-Triassic extinction horizon and multiple Hg/TOC peaks between it and the Triassic–Jurassic boundary is further evidence that pulses in the intensity of CAMP volcanism (and associated volatile release) were not limited to North America and Morocco, but representative of the entire province. The direct correlation between the oldest preserved flows of CAMP and the end-Triassic extinction horizon allows the earliest pulse of elevated mercury in the sedimentary record of this time to be linked directly with these basalts. This correlation supports a volcanic origin for the increased mercury abundances, and represents the first time that a globally observed mercury excursion has been tied to a specific basalt unit from a Large Igneous Province. The recording of multiple Hg/TOC excursions between the extinction horizon and the Triassic–Jurassic boundary highlights that the initial stages of CAMP emplacement were marked by multiple episodes of volcanic volatile release. Repeated volcanically driven perturbations of the ocean-atmosphere system in the 100–200 kyr during and immediately following the end-Triassic extinction may have had important implications for the biospheric impact of CAMP.

Methods

Mercury analysis was undertaken on the RA-915 Portable Mercury Analyzer with PYRO-915 Pyrolyzer, Lumex, at the University of Oxford (26). Where previous TOC determinations were not available, new data were measured using either a Strohlein Coulomat 702 (46) or Rock-Eval VI (47) at the University of Oxford. $\delta^{13}C_{org}$ analyses were performed on decarbonated Arroyo Malo samples (prepared at the University of Oxford) with a Thermo Scientific Flash 2000 HT Elemental Analyzer (EA) coupled to a Thermo Scientific

MAT253 isotope-ratio mass spectrometer via a Conflo IV open-split interface at the Stable Isotope Laboratory at the Open University (Milton Keynes, UK). For full method details, see Supplementary Information S1.

Acknowledgements

We gratefully acknowledge Alberto Riccardi, Susana Damborenea and Miguel Manceñido for their assistance in collecting material from Arroyo Malo, Argentina, Paul Olsen for assistance in collecting samples from Igounane, Morocco, and John Farmer and the University of Edinburgh for provision of geochemical standards. We greatly appreciate the two anonymous reviewers for their reviews, which much improved this manuscript. We acknowledge NERC (grant NE/G01700X/1 and PhD studentship NE/L501530/1), Shell International Exploration and Production Inc., a Niels Stensen Foundation Research Grant to Micha Ruhl, the US National Science Foundation (EAR 0801138 and EAR 1349650 to Jessica Whiteside), and the Leverhulme Trust for funding.

References

1 Schoene, B. *et al*., 2010, Correlating the end-Triassic mass extinction and flood basalt volcanism at the 100ka level. Geology, 38, p. 387–390, doi:10.1130/G30683.1.

2 Blackburn, T.J. *et al*., 2013, Zircon U-Pb Geochronology Links the End-Triassic Extinction with the Central Atlantic Magmatic Province. Science, 340, p. 941–945, 1234204, doi:10.1126/science1234204.

3 Raup, D.M. and Sepkoski, J.J., 1982, Mass Extinction in the Marine Fossil Record. Science, 215, p. 1501–1503, doi:10.1126/science.215.4539.1501.

4 Olsen, P.E. *et al*., 1987, New early Jurassic tetrapod assemblages constrain Triassic–Jurassic tetrapod extinction event. Science, 237, p. 1025–1029, doi:10.1126/science.3616622.

5 Olsen, P.E. *et al*., 1990, The Triassic/Jurassic boundary in continental rocks of eastern North America; A progress report. Geological Society of America Special Publications, 247, p. 585–594, doi:10.1130/SPE247-p585.

6 McElwain, J.C. *et al*., 1999, Fossil Plants and Global Warming at the Triassic–Jurassic Boundary. Science, 285, p. 1386–1390, doi:10.1126/science.285.5432.1386.

7 McElwain, J.C. *et al*., 2009, Fossil Plant Relative Abundances Indicate Sudden Loss of Late Triassic Biodiversity in East Greenland. Science, 324, p. 1554–1556, doi:10.1126/science.1171706.

8 Bonis, N.R. *et al*., 2009, A detailed palynological study of the Triassic–Jurassic transition in key sections of the Eiberg Basin (Northern Calcareous Alps, Austria). Review of Palaeobotany and Palynology, 156, p. 376–400, doi:10.1016/j.revpalbo.2009.04.003.

9 Hillebrandt A.v. *et al*., 2013, The Global Stratotype Sections and Point (GSSP) for the base of the Jurassic System at Kuhjoch (Karwendel Mountains, Northern Calcareous Alps, Tyrol, Austria). Episodes, 36, p. 162–198.

10 Hesselbo, S.P. *et al*., 2002, Terrestrial and marine extinction at the Triassic–Jurassic boundary synchronized with major carbon-cycle perturbation: A link to initiation of massive volcanism? Geology, 30, p. 251–254, doi:10.1130/0091-7613(2002)030<0251:TAMEAT>2.0.CO;2.

11 Ruhl, M. *et al*., 2009, Triassic–Jurassic organic carbon isotope stratigraphy of key sections in the western Tethys realm (Austria). Earth and Planetary Science Letters, 281, p. 169–187, doi:10.1016/j.epsl.2009.02.020.

12 Whiteside, J.H. *et al*., 2010, Compound-specific carbon isotopes from Earth's largest flood basalt eruptions directly linked to the end-Triassic mass extinction. Proceedings of the National Academy of Sciences, 107, p. 6721–6725, doi:10.1073/pnas.1001706107.

13 Bartolini, A. *et al*., 2012, Disentangling the Hettangian carbon isotope record: Implications for the aftermath of the end-Triassic mass extinction. Geochemistry, Geophysics, Geosystems, 13, Q01007, doi:10.1029/2011GC003807.

14 Deenen, M.H.L. *et al*., 2010, A new chronology for the end-Triassic mass extinction. Earth and Planetary Science Letters, 291, p. 113–125, doi:10.1016/j.epsl.2010.01.003.

15 Dal Corso, J. *et al*., 2014, The dawn of CAMP volcanism and its bearing on the end-Triassic carbon cycle disruption. Journal of the Geological Society, London, 171, p. 153–164, doi:10.1144/jgs2013-063.

16 Marzoli, A. *et al*., 1999, Extensive 200-Million-Year-Old Continental Flood Basalts of the Central Atlantic Magmatic Province. Science, 184, p. 616–618, doi:10.1126/science.284.5414.616.

17 El Ghilani, S. *et al*., 2017, Environmental implication of subaqueous lava flows from a continental Large Igneous Province: Examples from the Moroccan Central Atlantic Magmatic Province (CAMP). Journal of African Earth Sciences, 127, p. 211–221, doi:10.1016/j.afrearsci.2016.07.021.

18 El Hachimi, H. *et al*., 2011, Morphology, internal architecture and emplacement mechanisms of lava flows from the Central Atlantic Magmatic Province (CAMP) of Argana Basin (Morocco). Geological Society of London Special Publications, 377, p. 167–193, doi:10.1144/SP357.9.

19 Marzoli, A. *et al*., 2004, Synchrony of the Central Atlantic magmatic province and the Triassic–Jurassic boundary climatic and biotic crisis. Geology, 32, p. 973–976, doi:10.1130/G20652.1.

20 Olsen, P.E. *et al*., 1996, High-resolution stratigraphy of the Newark rift basin (early Mesozoic, eastern North America). Geological Society of America Bulletin, 108, p. 40–77, **doi:** 10.1130/0016-7606(1996)108<0040:HRSOTN>2.3.CO;2.

21 Kent, D.V. *et al*., 2017, Astrochronostratigraphic polarity time scale (APTS) for the Late Triassic and Early Jurassic from continental sediments and correlation with standard marine stages. Earth Science Reviews, 166, p. 153–180, doi:10.1016/j.earscirev.2016.12.014.

22 Schaller, M.F. *et al*., 2011, Atmospheric PCO_2 Perturbations Associated with the Central Atlantic Magmatic Province. Science, 331, p. 1404–1409, doi:10.1126/science.1199011.

23 Steinthorsdottir, M. *et al*., 2011, Extremely elevated CO_2 concentrations at the Triassic/Jurassic boundary. Palaeogeography, Palaeoclimatology, Palaeoecology, 308, p. 418–432, doi:10.1016/j.palaeo.2011.05.050.

24 Pyle, D.M., and Mather, T.A., 2003, The importance of volcanic emissions in the global atmospheric mercury cycle. Atmospheric Environment, 37, p. 5115–5124, doi:10.1016/j.atmosenv.2003.07.011.

25 Blum, J.D. *et al*., 2014, Mercury isotopes in earth and environmental sciences. Annual Review of Earth and Planetary Sciences, 42, p. 249–269, doi:10.1146/annurev-earth-050212-124107.

26 Sanei, H. *et al*., 2012, Latest Permian mercury anomalies. Geology, 40, p. 63–66, doi:10.1130/G32596.1.

27 Percival, L.M.E. *et al*., 2015, Globally enhanced mercury deposition during the end-Pliensbachian and Toarcian OAE: A link to the Karoo–Ferrar Large Igneous Province. Earth and Planetary Science Letters, v. 428, p. 267–280, doi:10.1016/j.epsl.2015.06.064.

28 Percival, L.M.E. *et al*., 2016, Osmium-isotope evidence for two pulses of increased continental weathering linked to volcanism and climate change during the Early Jurassic. Geology, 44, p. 759–762, doi:10.1130/G37997.1.

29 Font, E. *et al*., 2016, Mercury anomaly, Deccan volcanism, and the end-Cretaceous mass extinction. Geology, 44, p. 171–174, doi:1130/G37451.1.

30 Benoit, J.M. *et al*., 2001, Constants for mercury binding by dissolved organic matter isolates from the Florida Everglades. Geochimica and Cosmochimica Acta, 65, p. 4445–4451, doi:10.1016/S0016-7037(01)00742-6.

384 31 Outridge, P.M. *et al*., 2007, Evidence for control of mercury accumulation in sediments by variations of
385 aquatic primary productivity in Canadian High Arctic lakes. Environmental Science and Technology,
386 41, p. 5259–5265, doi:10.1021/es070408x
387
388 32 Benoit, J.M. *et al*., 1999, Sulfide Controls on Mercury Speciation and Bioavailability to Methylation
389 Bacteria in Sediment Pore Waters. Environmental Science and Technology, 33, p. 951-957,
390 doi:10.102/es9808200.
391
392 33 Niessen, S. *et al*., 2003, Influence of sulphur cycle on mercury methylation in estuarine sediment (Seine
393 estuary, France). Journal de Physique IV, 107, p. 953–956, doi:10.1051/jp:20030456
394
395 34 Kongchum, M. *et al*., 2011, Relationship between sediment clay minerals and total mercury. Journal of
396 Environmental Science and Health, Part A, 46, p. 534–539, doi:10.1080/10934529.2011.551745.
397
398 35 Thibodeau, A.M. *et al*., 2016, Mercury anomalies and the timing of biotic recovery following the end-
399 Triassic mass extinction. Nature Communications, 7, doi:10.1038/ncomms11147.
400
401 36 Tanner, L.H. *et al*., 2004, Assessing the record and causes of Late Triassic extinctions. Earth Science
402 Reviews, 65, p. 103–139, doi:10.1016/S0012-8252(03)00082-5.
403
404 37 Ruhl, M. *et al*., 2010, Sedimentary organic matter characterization of the Triassic–Jurassic boundary GSSP
405 at Kuhjoch (Austria). Earth and Planetary Science Letters, 292, p. 17–26,
406 doi:10.1016/j.epsl.2009.12.046.
407
408 38 Svensen, H. *et al*., 2009, Siberian gas venting and the end-Permian environmental crisis. Earth and
409 Planetary Science Letters, 277, p. 490–500, doi:10.1016/j.epsl.2008.11.015.
410
411 39 Ganino, C. and Arndt, N.T., 2009, Climate changes caused by degassing of sediments during the
412 emplacement of large igneous provinces. Geology, 37, p. 323–326, doi: 10.1130/G25325A.1.
413

414 40 Beerling, D.J. and Berner, R.A., 2002, Biogeochemical constraints on the Triassic–Jurassic boundary
415 carbon cycle event. Global Biogeochemical Cycles, 16, 1036, doi:10.1029/2001GB001637.
416
417 41 Whiteside, J.H. *et al*., 2007, Synchrony between the Central Atlantic magmatic province and the Triassic–
418 Jurassic mass-extinction event? Palaeogeography, Palaeoclimatology, Palaeoecology, 244, p. 345–
419 367, doi:10.1016/j.palaeo.2006.06.035.
420
421 42 Xu, W. *et al*., 2017, Orbital pacing of the Early Jurassic carbon cycle, black-shale formation and seabed
422 methane seepage. Sedimentology, 64, p. 127–149, doi:10.1111/sed.12329.
423
424 43 Self, S. *et al*., 2014, Emplacement characteristics, time scales, and volatile release rates of continental
425 flood basalt eruptions on Earth. In: Keller, G., Kerr A. (Eds.), Volcanism, Impacts and Mass
426 Extinctions: Causes and Effects. Geological Society of America Special Paper 505, p. 319–338,
427 doi:10.1130/2014.2505(16).
428
429 44 Schmidt, A. *et al*., 2015, Selective environmental stress from sulphur emitted by continental flood basalt
430 eruptions. Nature Geoscience, 9, p. 77–82, doi:10.1038/ngeo2588.
431
432 45 Ritterbush, K.A. *et al*., 2015, Andean sponges reveal long-term benthic ecosystem shifts following the end-
433 Triassic mass extinction. Palaeogeography, Palaeoclimatology, Palaeoecology, 420, p. 193–209,
434 doi:10.1016/j.palaeo.2014.12.002.
435
436 46 Jenkyns, H.C., 1988, The early Toarcian (Jurassic) anoxic event: Stratigraphic, sedimentary, and
437 geochemical evidence. American Journal of Science, 288, p. 101–151, doi:10.2475/ajs.288.2.101.
438
439 47 Espitalié, J. *et al*., 1977, Source rock characterization methods for petroleum exploration. Proceedings of
440 the 1977 Offshore Technology Conference, 3, p. 439–443.
441
442 48 Kent, D.V. and Olsen, P.E., 1999 Astronomically tuned geomagnetic polarity timescale for the Late
443 Triassic. Journal of Geophysical Research, 104, p. 12831–12841, doi:10.1029/1999JB900076.

49 Olsen, P.E. *et al*., 2002, Ascent of Dinosaurs Linked to an Iridium Anomaly at the Triassic-Jurassic Boundary. Science, 296, p. 1305–1307, doi:10.1126/science.1065522.

50 Ruhl, M. *et al*., 2010, Astronomical constraints on the duration of the early Jurassic Hettangian stage and recovery rates following the end-Triassic mass extinction (St Audrie's Bay/East Quantoxhead, UK). Earth and Planetary Science Letters, 295, p. 262–276, doi:10.1016/j.epsl.2010.04.008.

51 Bonis, N.R. *et al*., 2010, Milankovitch-scale palynological turnover across the Triassic–Jurassic transition at St. Audrie's Bay, SW UK. Journal of the Geological Society, London, 167, p. 877–888, doi:10.1144/0016-76492009-141.

52 Hounslow, M.W. *et al*., 2004, Magnetostratigraphy and biostratigraphy of the upper Triassic and lowermost Jurassic succession, St Audrie's Bay, UK. Palaeogeography Palaeoclimatology Palaeoecology, 213, p. 331–358, doi:10.1016/j.palaeo.2004.07.018.

53 Hüsing, S.K. *et al*., 2014, Astronomically-calibrated magnetostratigraphy of the Lower Jurassic marine successions at St. Audrie's Bay and East Quantoxhead (Hettangian–Sinemurian; Somerset, UK). Palaeogeography Palaeoclimatology Palaeoecology, 403, p. 43–56, doi:10.1016/j.palaeo.2014.03.022.

54 Riccardi, A.C. *et al*., 2004, The Triassic/Jurassic boundary in the Andes of Argentina. Rivista Italiana di Paleontologia e Stratigrafia, 110, p. 69–76, doi:10.13130/2039-4942/6266.

55 Deenen, M.H.L. *et al*., 2011, The quest for E23r at Partridge Isalnd, Bay of Fundy, Canada: CAMP emplacement postdates the end-Triassic extinction event at the North American craton. Canadian Journal of Earth Sciences, 48, p. 1282–1291, doi:10.1139/e11-015.

Figure Captions:

Figure 1: A: Stratigraphic correlation of the end-Triassic extinction with the Moroccan Lower Formation CAMP basalt. Argana lithology, carbon-isotope, and paleomagnetic data are from 14. Newark lithology and pCO_2 data are from 22, paleomagnetic and astrochronological data are from 48; carbon-

isotope data from 12; trilete spore data from 49. St Audries Bay lithology and astrochronology are from 42 and 50, biostratigraphy and carbon-isotope data from 10 and 50, trilete spore data from 51, paleomagnetic data from 52 and 53. Stratigraphic correlation of CAMP units between Argana, Newark, and St Audries Bay is based on 12 and 42. Kuhjoch biostratigraphy, lithology, and carbon-isotope data are from 11. The end-Triassic extinction horizon (marked as ETE) and Triassic–Jurassic boundary (marked as TJB) are also shown. **B:** Example of new Hg/TOC data from this study (Kuhjoch, Figure 3) are shown to stratigraphically correlate with the lowest CAMP basalt unit that intersects the end-Triassic extinction at Argana. See Supplementary Figure S2 for a full stratigraphic correlation of end-Triassic records.

Figure 2: A: Paleogeographic reconstruction of the end-Triassic world, with the modern continents overlain. The locations of the six studied sections are indicated (A: St Audries Bay, UK; B: Kuhjoch, Austria; C: Arroyo Malo, Argentina; D: Astartekløft, Greenland; E: Partridge Island, Canada; F: Igounane, Morocco). The New York Canyon section in Nevada, USA (G: note different color) studied by 35, and the Central Atlantic Magmatic Province (CAMP) are also shown (based on Figure 1 from ref 2). **B:** Summarized composite stratigraphy of Moroccan and North American CAMP basalts, following the stratigraphic relationships and ages (in Myrs) from 2 and 14. The Hickory Grove basalt is included with the Preakness due to their geochemical similarity. The age of the end-Triassic extinction (marked as ETE) is also indicated.

Figure 3: Comparison of Hg/TOC data from St Audries Bay, Kuhjoch, Arroyo Malo, Astartekløft, and New York Canyon (35), and Hg data from Partridge Island and Iguonane (where TOC contents were below error). Carbon-isotope data, biostratigraphy (ammonite First Appearance), lithology, and magnetostratigraphy are also shown to allow stratigraphic correlation of the end-Triassic extinction horizon (marked as ETE) and Triassic–Jurassic boundary (marked as TJB). Lithological data is from St Audries Bay (10), Kuhjoch (11), Arroyo Malo (54), Astartekløft (10), Partridge Island (this study; shown in figure), Argana (14), Igouane (this study; shown in figure) and New York Canyon (35). Carbon-isotope and biostratigraphic data is form St Audries Bay (10 and 50), Kuhjoch (11), Arroyo Malo (54 and this study), Astartekløft (10), Partridge Island (this study), Argana (14) and New York Canyon (35). Line M indicates the magnetostratigraphic correlation, below the extinction horizon, between St Audries Bay, Partridge Island, Argana, and Igounane. The gray shading illustrates the

stratigraphic gap between line M and line ETE. Magnetostratigraphic data is from St Audries Bay (52 and 53), Partridge Island (55) and Argana (14). Note for Astartekløft the expanded horizontal scale, and the gaps in data due to sand beds with negligible TOC. Full $\delta^{13}C$, Hg, TOC and Hg/TOC data for each individual section are reported in the Supplementary Tables S3 and Supplementary Figure S4. (For interpretation of the references to color in this figure, the reader is referred to the web version of this article).

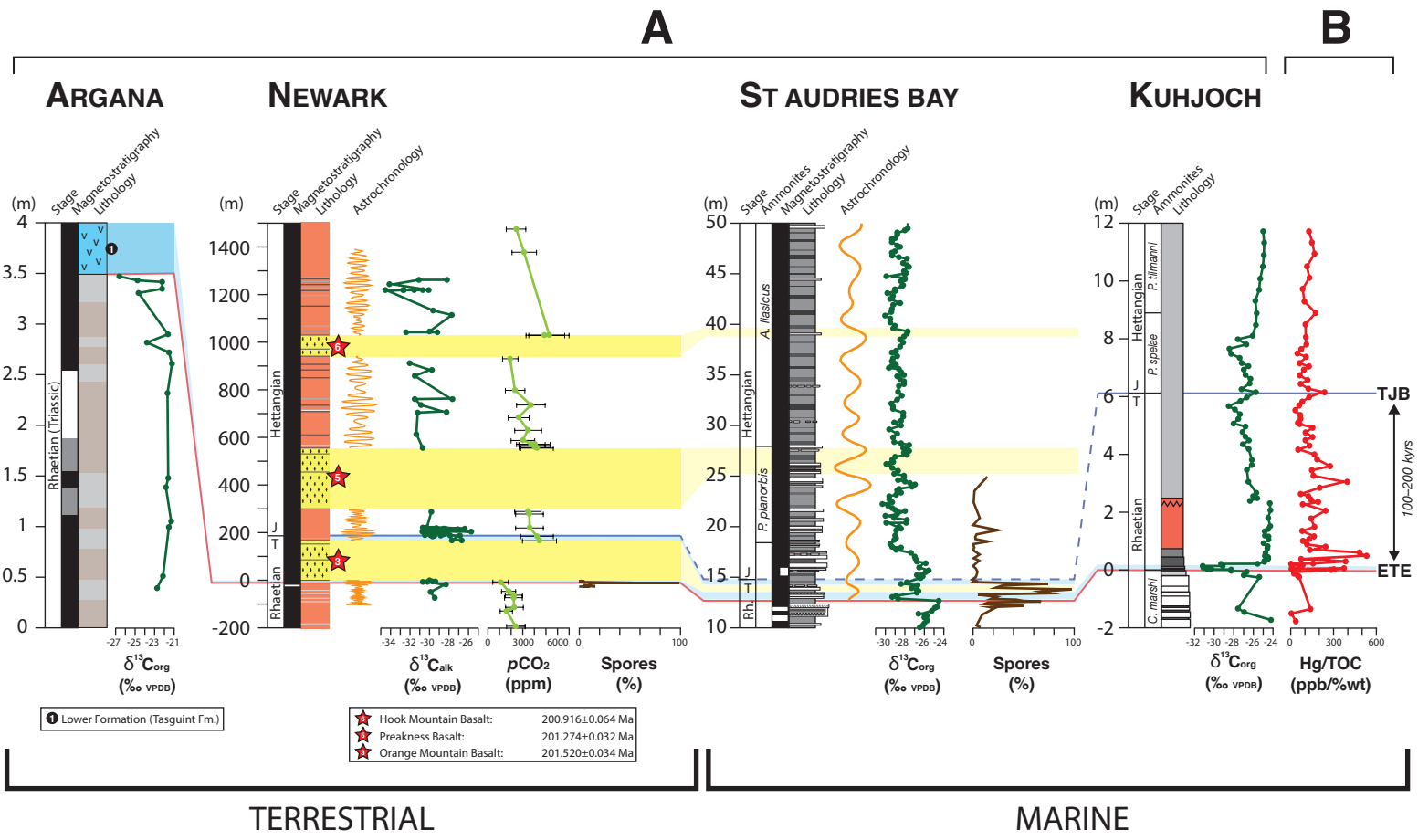
A
B
ARGANA
NEWARK
ST AUDRIES BAY
KUHJOCH
Stage
Magnetostratigraphy
Lithology
Astrochronology
Ammonites
(m)
Rhaetian (Triassic)
Hettangian
Rhaetian
Rh.
J
T
A. liasicus
P. planorbis
P. tilmanni
P. spelae
C. marshi
TJB
ETE
100–200 kyrs
δ13Corg (‰ VPDB)
δ13Calk (‰ VPDB)
pCO2 (ppm)
Spores (%)
Hg/TOC (ppb/%wt)
1 Lower Formation (Tasguint Fm.)
Hook Mountain Basalt: 200.916±0.064 Ma
Preakness Basalt: 201.274±0.032 Ma
Orange Mountain Basalt: 201.520±0.034 Ma
TERRESTRIAL
MARINE

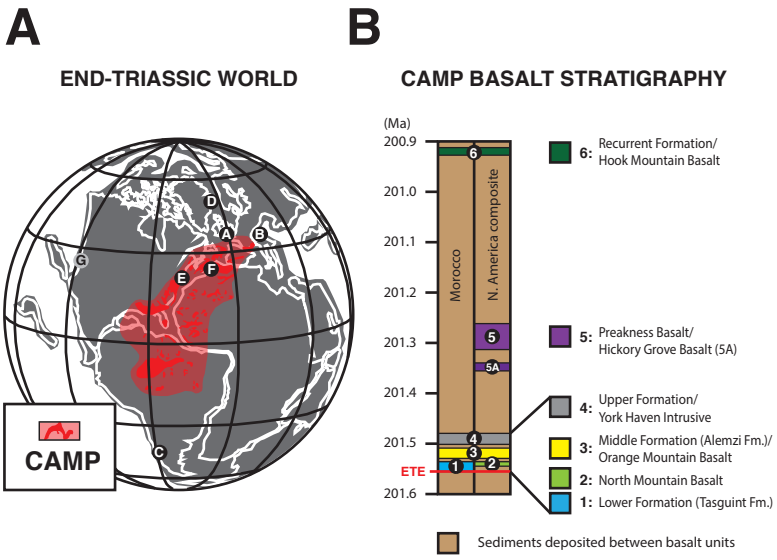
A
END-TRIASSIC WORLD
CAMP
A
B
C
D
E
F
G
B
CAMP BASALT STRATIGRAPHY
(Ma)
200.9
201.0
201.1
201.2
201.3
201.4
201.5
ETE
201.6
Morocco
N. America composite
6
5
5A
4
3
2
1
6: Recurrent Formation/ Hook Mountain Basalt
5: Preakness Basalt/ Hickory Grove Basalt (5A)
4: Upper Formation/ York Haven Intrusive
3: Middle Formation (Alemzi Fm.)/ Orange Mountain Basalt
2: North Mountain Basalt
1: Lower Formation (Tasguint Fm.)
Sediments deposited between basalt units

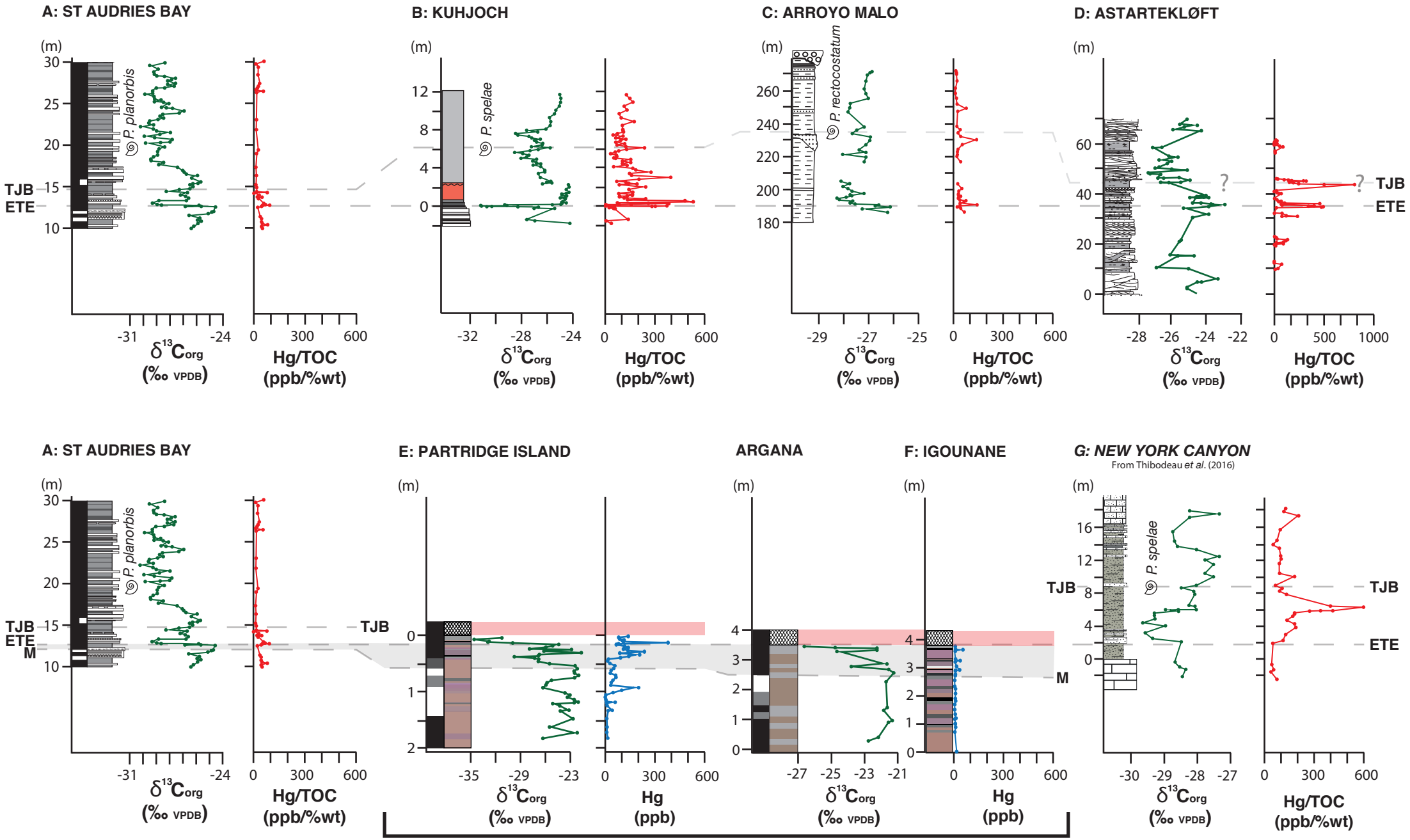
A: ST AUDRIES BAY
B: KUHJOCH
C: ARROYO MALO
D: ASTARTEKLØFT
(m)
P. planorbis
P. spelae
P. rectocostatum
TJB
ETE
δ13Corg (‰ VPDB)
Hg/TOC (ppb/%wt)
A: ST AUDRIES BAY
E: PARTRIDGE ISLAND
ARGANA
F: IGOUNANE
G: NEW YORK CANYON
From Thibodeau et al. (2016)
M
Hg (ppb)
Lithology*:
CAMP basalt
Mudstones (color indicates the color of the mud in outcrop)
*Applicable only at Partridge Island, Argana, and Igounane. Other lithological data sourced from previously published works (see figure caption).